

# **First-Generation Jet Propulsion Laboratory "Hockey-Puck" Free-Flying Magnetometers for Distributed *In-Situ* Multiprobe Measurement of Current Density Filamentation in the Northern Auroral Zone: Enstrophy Mission**

H. Javadi, B. Blaes, M. Boehm <sup>†</sup>, K. Boykins, J. Gibbs, W. Goodman <sup>\*</sup>, U. Lieneweg,  
J. Lux, K. Lynch <sup>@</sup>, P. Narvaez, M. Quadrelli, D. Perrone, B. Snare, H. Spencer, M. Sue, B. Thoma,  
J. Willis, J. Weese, K. Leschly, and R. Goldstein

Jet Propulsion Laboratory, California Institute of Technology, Pasadena, CA

<sup>†</sup>Lockheed Martin ATC, Palo Alto, CA

<sup>\*</sup>Applied Physics Systems, Inc., Mountain View, CA

<sup>@</sup>University of New Hampshire, Durham, NH

## **ABSTRACT**

The sub-orbital rocket mission was a collaborative project between the University of New Hampshire, Cornell University, and the Jet Propulsion Laboratory (JPL) to study filamentation phenomena in the northern Auroral zone. The Enstrophy mission test flew the JPL Free-Flying Magnetometer (FFM) concept. The FFM technology development task has been funded by NASA to develop miniaturized, low-power, integrated "sensorcrafts". JPL's role was to design, integrate, test, and deliver four FFMs for deployment from the sounding rocket, allowing a unique determination of curl-B. This provides a direct measurement of magnetic-field-aligned current density along the rocket trajectory.

A miniaturized three-axis fluxgate magnetometer was integrated with a 4-channel 22-bit sigma-delta Analog to Digital Converter (ADC), four temperature sensors, digital control electronics, seven (Li-SOCl<sub>2</sub>) batteries, two (4° x 170° field of view) sun-sensors, a fan-shaped-beam laser diode beacon, a (16 MHz) stable Temperature Compensated Crystal Oscillator (TCXO) clock, Radio Frequency (RF) communication subsystem, and an antenna for approximately 15 minutes of operation where data was collected continuously and transmitted in three (3) bursts (approximately 26 seconds each) to ground station antennas at Poker Flat, Alaska. FFMs were stowed within two trays onboard the rocket during the rocket launch and were released simultaneously using the spinning action of the rocket at approximately 300 km altitude (~100 sec. into the flight). FFMs were deployed with spin rate of ~17 Hz and ~3 m/sec linear velocity with respect to the rocket. For testing purposes while the rocket was in the launch pad and during flight prior to release of FFMs from the rocket, commands (such as "power on", "test", "flight", "power off", and clock "Reset" signal) were transmitted via an infrared Light Emitting Diode to an infrared detector in the FFM. Special attention was paid to low magnetic signature electronic design and choice of materials in packaging. The miniaturized fluxgate magnetometers had a range of 1-60000 nT with 0.1% full-scale linearity. The frequency range of interest for magnetic measurement was 10 mHz - 50 Hz. Digital data from the magnetometer's three axes were placed in a 4MB Static Random Access Memory (SRAM) in data packages (frames) formatted together with time tags and frame ID. After a specified time was elapsed, the data were Viterbi encoded and transmitted at a rate of 100 kbps (BPSK). Each of the four FFMs transmitted at different frequency. These carrier frequencies were in the range of 2200-2300 MHz. The antenna was a single patch on a high dielectric constant substrate covering one end-plate of the hockey-puck-sized unit. The local clocks aboard the FFMs were reset at the start of the mission and stayed synchronized within 3 msec during the mission. Position of each FFM with respect to the rocket is calculated by the knowledge of its release velocity (measured at exit point of the FFM launcher tract) providing an accuracy of 1 m over the maximum range of 3 km. Spatial and temporal nature of observants can be separated to within 3 m in space or 3 msec time interval.

**Keywords:** microspacecraft, nanospacecraft, sciencecraft, free flying magnetometer, free flyer, multiprobe measurement, cluster class mission, planetary magnetosphere.

Further author information -

H. Javadi: Email: hamid.h.javadi@jpl.nasa.gov; Telephone: 818-354-5655; FAX: 818-393-6875

## Introduction

The Enstrophy mission was proposed jointly by the University of New Hampshire, Cornell University, and the Jet Propulsion Laboratory (JPL) to NASA in response to the Space Physics NRA of 1996 (PI: Prof. Kristina Lynch). Its goal was to make multiple-point measurement of the magnetic field in the northern auroral zone via four small free-flyers. The results will be used to calculate magnetic-field-aligned current density along the rocket trajectory. The mission technical objective was the proof of concept of the JPL FFM design. The scientific goal was to study the structure of small-scale current systems in the nightside auroral region.

The four FFMs were deployed successfully from a sub-orbital rocket launched from the Poker Flat, Alaska range at about 10:00 PM local time on 2/10/99. Full data were obtained from three FFMs (partially from the 4th FFM) during all three transmission periods. These hockey-puck-sized "sciencecrafts" (80 mm diameter, 38 mm height, 250 gram mass) each carried a miniaturized 3-axis fluxgate magnetometer for field measurement, two sun sensors for attitude determination, a fan-shaped-beam diode laser which enabled FFM attitude determination relative to the spinning rocket at night, seven Lithium Thionyl Chloride batteries, an integrated data subsystem, and a miniaturized S-band transmitter for direct communication to the ground station antennas near the launch pad. The magnetic signatures of the electronic and mechanical materials within the FFM were screened to satisfy the FFM magnetometer sensitivity requirements. The FFMs were stowed inside the rocket platform before being released. At an altitude of ~300 km, they were ejected simultaneously perpendicular to the rocket approximately 90 degrees apart from each other. The FFMs were designed for inertial stability within the constraint of the mission and were tested for dynamic spin balance before launch. In addition to the JPL FFMs, the rocket carried other instrumentations from Cornell University and the University of New Hampshire.

We will describe the realization of the first FFM microspacecraft as intended for a specific NASA mission. Details related to the Enstrophy mission and its scientific achievements will be reported in the future[1-3].

## Enstrophy Mission

A three-stage Black Brant - 10 rocket (Terrier, Black Brant - 5C, Nihka) was used in the Enstrophy Mission. The rocket did not carry any attitude control system for weight reduction (and also for rigid-body-motion of main payload for data analysis of main payload magnetometer data) and it reached altitude of 1070 km. The rocket spun at high rate of 6 Hz while the FFMs were ejected from the rocket at an altitude of ~300 km. Design of the ejection mechanism was based on roll (no slip) motion of each FFM within its individual spiral-shaped tract. The FFMs were originally held in the rocket with a spring loaded stopper. Soon after the stopper was removed from the paths, the FFMs started rolling under the combined effect of coriolis and centrifugal force. Two FFMs were stowed between two trays stacked perpendicular to the axis of the rocket and left the rocket exactly on the opposite ends of its diameter. The other two FFMs were kept right above them in separate trays with their exit openings rotated 90 degrees with respect to the lower trays. The linear velocity of FFMs departing the rocket were about 3 m/sec. The FFMs followed the rocket trajectory while they were continuously separating from the rocket. The rocket carried some additional science instruments to complement the measurements of the FFM magnetometers. The FFMs transmitted their data directly to ground station antennas. Commercial receivers and bit synchronizers were employed in the ground station to receive the FFM data. Two ground station antennas were employed (8m and 11m diameters). The received data were stored on digital and analog magnetic tapes and also were acquired by a lap-top computer. An IR transmitter inside the rocket platform was used to send special commands to each FFM IR receiver in order to turn the FFM power on and start the test mode for nightly vertical test before the final rocket lift-off. Other commands for FFM clock reset, and to start FFM flight mode were also communicated via the IR interface after the rocket lift-off. All FFM clocks were reset right before their ejection from the rocket. This was necessary to cross-correlate the external events as were recorded by the magnetometers onboard different FFMs. Attitude determination of each FFM is made possible via two onboard sun sensors ( $4^\circ \times 170^\circ$  field of view). Sun was only visible at high altitudes as the rocket was launched at approximately 10:00 pm local time. Another scheme is implemented to obtain attitude information while in dark; each FFM carries a (85 degrees) fan-shaped-beam laser beacon with the beam in the plane of FFM axis looking radially outward. As the FFM spins, the fan beam sweeps space past the rocket. A single array of sensitive optical detectors mounted on the side of the rocket provided information on the attitude of the FFM with respect to the rocket. The rocket's attitude in turn is obtained via star sensor, horizon sensor, and main payload magnetometer.

The Enstrophy mission subsystem-level block diagram is shown in Fig. 1. This paper will describe the design, manufacturing, and test of the FFM units. We will discuss briefly those instruments onboard the rocket which interfaced with the FFMs. In other publications we will report on the Enstrophy mission specifics[2], the FFM data reduction[3], FFM digital subsystem[4] and flight system development.

## Free-Flying Magnetometer

The Free-Flying Magnetometer microspacecraft was designed for the specific needs of the Enstrophy mission. Its miniaturized 3-axis fluxgate magnetometer acquired the data and provided an analog output for each of its axes. The analog signals were interfaced to first three channels of a ADC. The fourth channel input of the ADC was connected to a multiplexer sampling temperature sensors and other system health monitoring probes. The heart of the FFM was an FPGA-based digital electronics interfacing with onboard sensors (magnetic, temperature, sun sensor), memories [Electrically Erasable Programmable Read Only Memory (EEPROM), and SRAM], IR umbilical command communication, clock [Temperature Compensated Crystal Oscillator (TCXO)], and output subsystems (laser beacon and RF communication subsystem). Upon the receipts of "Power on" and "Flight" commands via the umbilical interface, the FPGA was powered. It went through some initiation routines; it loaded the program codes from the EEPROM, and turned on the magnetometer and sun sensors. The digital data outputs from the 4 channels of the ADC were stored in a 4 MB SRAM. At the end of approximately 5 minutes data gathering, the data was fetched from the SRAM, formatted to Non-Return-to-Zero (NRZ-M) and Viterbi encoded ( $K=7, 1/2$ ), and was sent to the S-band transmitter. All the electronics onboard this unit ran from a single clock, so no low-frequency signal would have been generated (because of frequency beatings between multiple clocks) which may have corrupted the sensitive magnetometer.

A block Diagram of the FFM unit is shown in Fig. 2 with its mechanical structure envelope in Fig. 3. Details of subsystem design and test are discussed below.

### FFM Integrated Data Subsystem

The FFM data subsystem design encompassed both analog and digital electronics and it included power regulation and management, ADC, and FPGA-based control and data flow management. The ADC was a high resolution, 22-bit 4-channel  $\Sigma$ - $\Delta$  converter with noise specified at 11  $\mu$ Vrms max (useable dynamic range is 108 dB or slightly more than 17 bits when cutoff frequency is 73 Hz). The ADC chip (Analog Devices AD7716) has an internal digital filter. The output rate was chosen to be 279 words/sec. As only one out of every two data points was taken, there existed a roll-off at  $279/2 = 69.75$  Hz. The digital filter settle time was 10.8 msec. The ADC data output has two's complement format. Channels 1-3 were connected to the magnetometer X, Y, and Z outputs (2 V maximum signal voltage). Channel 4 measured the output of four temperature sensors. One temperature sensor was mounted on the magnetometer PCB and was glued to the magnetometer core, the other was mounted on the magnetometer PCB, the third was glued to the TCXO, and the fourth was mounted on the analog board in the vicinity of the ADC. Channel 4 also monitored three supply voltages and a voltage baseline. The FPGA was a 13000 gate count chip in a plastic package (Xilinx, XC4013-E). The data from sun sensors occupied five subframes in the data package (16-bit word). Each data frame had a total of 64 words and started with two synchronization words (total overhead 3%). It had a frame ID, time tag (1  $\mu$ sec resolution) and a FFM-unit ID (to identify data). The FFM units were distinguishable by their transmission frequencies. The data from ADC channels 1-3 were saved in 17-bit value (16 consecutive measurements of 3-axis data was stored in 51 words). The ADC maximum input voltage was  $\pm 2.5$  V. The Lowest Significance Bit (LSB) in the stored digital data thus corresponded to slightly more than 1 nT. A 4 Mbit SRAM was used to store the 2547 frames of data in each data acquisition / transmission cycle. The FFM required  $\sim 26$  seconds to transmit stored data at the rate of 100 kbps. Each transmission was preceded by 15 sec of carrier-only broadcast to allow the receiver to lock up to the transmitter carrier frequency.

External IR transmitters onboard the rocket transmitted commands to each FFM via the IR receiver circuitry. A total of 4 commands were distinguishable which were "Power On", "Test", "Flight", "Power Off". The IR receiver must receive two consecutive broadcasts of the same 5-bit address plus 4-bit command pattern before being recognized as valid. The IR receiver circuit introduced  $\sim 120$  msec maximum delay. In order to guarantee a phase matched response to the "Reset" signal between all 4 FFMs, the IR decoder was bypassed. The "Test" mode was used for nightly vertical test of FFMs while still inside the rocket. During this mode, Each FFM measured about 100 frames of data and transmitted the data back to the main antenna at Poker Flat. This was accomplished via a pick-up antenna inside the rocket which in turn carried the signal to another antenna at the skin of the rocket for transmission. Each FFM was automatically turned-off after the "Test" sequence but could have also been forced off at any time with the "Power Off" command. The FFM power was turned on right before lift-off of the rocket. At this point the FFMs transmitted carrier which was used to verify that the FFMs were powered. After approximately 100 seconds into the flight, The "Flight" command followed by a "Reset" pulse were sent to the FFMs. The "Reset" pulse zeroed the clocks onboard all the FFMs. The "Reset" pulse was originated from the 1 pulse-per-second output of a GPS receiver. After the "Reset" pulse, the FFMs entered their data acquisition / transmission cycle and were deployed from the payload (See Fig. 4).

## FFM Miniaturized Fluxgate Magnetometer

A miniaturized 3-axis high field fluxgate magnetometer was developed for the FFM. The magnetometer consisted of one toroidal core (with coil windings for X and Y axes) and one race-track shaped core placed in the middle of the toroidal one (with single coil winding along the Z-axis). The cores were made out of  $\text{Ni}_{0.83}\text{V}_{0.06}\text{Fe}_{0.11}$  compound with superior noise properties. The overall dimensions of the sensor core box were 13 x 13 x 16 mm. The magnetometer cores were driven to saturation by a 25 KHz signal. Second harmonic response was synchronously detected and amplified. An active filter (single pole with 3-dB cut-off at 100 Hz) was employed at the output. Drive electronics for the cores and the read-out electronics were implemented on two PCBs (Figure 5). Commercial off-the-shelf electronic components were used.

Applied Physics Systems (Mountain View, CA) under a contract from JPL developed this miniaturized 3-axis fluxgate magnetometer with the following characteristics:

- Maximum signal:	+/- 60,000 nT
- Orthogonality range (typical):	1 - 3 degree (+0.5 degree error)
- Sensitivity:	2.0 V / 60000 nT
- Magnetic noise level (typical):	<0.06nT rms/sqrt(Hz) at 1 Hz, 1/f below 1 Hz
- Frequency response (typical):	DC to 100 Hz (3 dB)
- Linearity:	<0.1% FS
- Temperature coefficient:	strong temperature dependences (is modified with proper thermal packaging)
- Drift (typical):	< 20 nT / 20 min. < 2 nT/1 min. < ~0.3 nT/1 sec.
- Power consumption (typical):	+3V @ 60 mA -3V @ 60 mA
- Size (cylindrical):	38 mm diameter x 17 mm long
- Packaging:	
• thermal design:	• extended ground plane PCBs, upper PCB thermally is connected to the magnetometer cores.
• mechanical design:	• provides coordinate references

**Table 1**

There were larger nonlinearity at magnetic fields > 50000 nT as the amplifiers ran closer to the voltage supply rails. Outputs of the magnetometer were directly connected to channels 1-3 of the ADC (1 nT corresponds to 33  $\mu\text{V}$ ). Temperature dependence of the magnetometer drift and scale factor was of concern. A thermal analysis of near-final FFM package was done. We assumed Earth IR heating on the FFM antenna and the FFM shell cylindrical side with the opposite endplate looking into cold sky. The calculations showed that near final thermal configuration with the magnetometer top PCB thermally isolated from the core (starting at initial temperature of 25° C) and counting power dissipations of the FFM subsystems, the thermal gradient across the top PCB is less than ~4° C reducing to ~2° C when magnetometer top PCB is thermally connected to the core.

One of the biggest challenges of the FFM project was integration of live electronics in close vicinity of a sensitive magnetometer. Our goal was to limit total DC interference of the electronics and packaging materials on the magnetometer to <1 nT in the frequency range of interest (10 mHz-100 Hz). All electronics components were screened for low magnetic signature. We avoided ceramic packages with Kovar leads, most RF connectors and semirigid cables, and large capacitors containing Ni in their metal electrodes. Non-magnetic A-286 steel was used in construction of the sun-sensor body. Magnetic signatures of all electronic components were degaussed before soldering onto the boards. The electronic boards were also degaussed before final assembly. DC magnetic fields of major current carrying traces on the FFM digital and analog boards were calculated at position of the magnetometer core. Careful routing of traces was made to minimize the interference. Calculations showed that the overall effect must be below 1 nT. In principle, constant DC magnetic field generated by the current traces in the layout can be calibrated out and its effect is minimum when measurements of magnetic field variations are of interest.

A typical FFM magnetometer noise power spectrum (while integrated with the FFM analog and digital boards but prior to integration with the FFM transmitter and batteries) was measured to be approximately  $(0.2/f) + 0.02 \text{ nT}^2 / \text{Hz}$ . This corresponds to a standard deviation of ~1.2 nT over the frequency band of interest. Detailed FFM magnetometer noise data will be reported in our future publications.

## FFM IR Command Receiver

Commands to power on or off the FFM's and to enter into the test or flight modes were communicated to each FFM through an IR channel. The transmitter design utilized a MC145026 encoder chip to generate serial data consisting of 4-bit data and a 5-bit address. A buffer was used to drive the IR LEDs with ~50 mA current. On the receiver side, the IR signal was detected by a PD481 photodiode, which triggered a low speed / power comparator and then was decoded by a MC145027. The "Reset" signal was also transmitted via the IR channel. The delay time through comparator / decoder was a strong function of IR signal level. In order to avoid matching all FFM's for this delay, the detected "Reset" signal bypassed the IR decoder and was sent to a high-speed comparator and then directly to the FFM digital subsystem. The "Reset" signal was not recognizable until the FFM was in "Flight" mode. To conserve battery life, the FFM IR command receiver required very little power (< 30  $\mu$ A from 7 Volt battery).

## FFM Laser Beacon

One of the largest technical problem for the Enstrophy mission was that of determining FFM attitude. The sun-sensors provided a good solution when the sun was in view of FFM's. FFM attitude determination at night was facilitated by using a laser diode with line-generator optics on each FFM, and corresponding linear photon-multiplying receivers on the rocket. The commercial laser had a 85° fan shaped beam with the laser beam divergence of ~0.3 mrad. The 670 nm diode laser had <3 mW total power when powered with a 5V supply. Each receiver on the rocket had a field of view of ~60° in the rocket's spin plane and ~10° in the perpendicular direction. A large area avalanche photodiode was used to detect the beam.

## FFM Transmitter & Antenna

The block diagram of the FFM transmitter is shown in Fig. 6. It consisted of a Voltage-Controlled Oscillator (VCO) (Vari-L VCO-2250T) phase locked to a 16 MHz TCXO (Cardinal Components, Inc. [5] CTCX-A4B4-16). Temperature dependence of the TCXO in the range of -10° C to +40° C is shown in Fig. 7 indicating +1 ppm total variation.

A National LMX2330A phase lock chip was utilized. The synthesized frequency was in the range allocated to space-Earth communications (2200-2300 MHz). The output of the synthesizer was fed to a phase-modulator chip (RF MicroDevices RF2422). The result was a Bi-Phase Shift Key (BPSK) carrier signal which was then amplified by a two-stage amplifier (RF2310 and RF2128P) to more than 20 mW level and fed to a single-patch antenna. The single-patch antenna on a 2 mm thick substrate (TMM6.060 Rogers Corp.) was designed and built by MicroPulse, Inc. [6] for the FFM project. A stripline hybrid was used for the antenna feed which was implemented on an FR-4 substrates. Two probes connected the hybrid feed to appropriate locations on the patch (Fig. 8). The performance data of the antenna is shown in Table 2.

- Center frequency:	2250 MHz
- Polarization:	RHCP
- VSWR (>1.5:1) BW:	80 MHz
- Circular Polarization BW:	80 MHz
- Axial Ratio:	< 4 dB across the full 60° half solid angle beamwidth
- Substrate thickness:	2 mm thick high- $\epsilon$ microwave substrate on top of a 1.5 mm thick PCB
- Diameter of antenna disk:	77 mm
- Antenna gain at nadir:	> 2 dB CP gain
- Antenna Pattern:	better than -3 dB gain (with respect to nadir) at 30° from the nadir better than -8 dB (with respect to nadir) at 60° from the nadir
- Feed:	single point feed at the edge of the antenna

Table 2

A typical antenna pattern is shown in Fig. 9. The antenna CP gain drops from 5 dB at nadir to -1 dB at 60° off, and to -2 dB at 90° off. Axial ratio represents antenna cross-polarization levels of -21 dB at nadir, -11 dB at 60° off and -7 dB at 90° off.

## FFM Batteries

High-capacity LiSOCl<sub>2</sub> batteries supported nearly 1.5 hours life span for a FFM unit. Typical dimensions of the LTC-312 (Eagle Picher Industries, Inc. [7]) battery were 2.5 x 17.5 x 37.1 mm. A typical full-load test (based on the FFM mission) is depicted in Fig. 10. The wide solid line is the voltage of a single battery under load and the narrow solid line is the current. This operational profile mimics worst-case load of the FFM batteries during the Enstrophy mission preparation, test, and

flight with additional margins. The shelf life of Lithium batteries is good due to build-up of a passivation layer on the Li electrode which prevents depletion of the charged capacity (~3% depletion/year). At the same time, this passivation layer requires a "work-in" of the battery before the mission. Before the current starts to break through the passivation layer, the voltage of the battery shows a drop. We needed to run some currents through the battery before the mission start in order to avoid FFM electronic circuits malfunction due to low voltage. This is labelled "work-in" and was considered for this mission. Functional tests prior to the Enstrophy rocket launch could work-in the batteries. Batteries (soaked at -20° C under 0.1 A load) provided the minimum voltage needed for the low-drop-out 5V regulators to function. A total of 3 pairs plus one single battery were needed to supply voltages for all FFM subsystems. The fluxgate magnetometer required +/-3 V at +/- 60 mA current and provided +/- 2.0 V full scale signal at X,Y,Z output ports. The transmitter required +5V. The data subsystem interfaced with magnetometer and transmitter and it managed power for the entire FFM unit.

### **FFM Sun Sensors**

The FFM prototype sun sensor was designed and tested at the US Army Research Laboratory[8]. Flight units were manufactured at JPL using non-magnetic materials and metal coatings. The FFM sun sensor had overall dimensions of 15.0 x 15.0 x 5.0 mm and utilized a new design of an optical slit with an obstructive pillar, smoothly curved reflectors and light absorbing ridges, and a miniature silicon solar cell. The sensor acted as a voltage/current source under incident light and thus did not need external power. The geometry and construction of the sun sensor is patent pending by personnel of the U.S. Army Research Laboratory. Two sun sensors were integrated with each FFM unit. They were mounted on the cylindrical wall of the FFM 180° apart looking radially outward with one sun sensor tilted by 30°. Figure 11 (12) shows typical output of the sun sensor when a light source swept across a plane perpendicular (parallel) to the slit and passed through the center of the slit opening. The field of view was thus 4° x 170° for a 20% maximum amplitude threshold. The tilted sun sensor allowed a measurement range of approximately 40° to 140° degrees for a 170° field of view and 20% threshold (90° is normal to the slit opening plane). Combination of two sun sensors (one 30° tilted) provided additional information about the FFM angular motion.

### **FFM Mechanical Packaging**

Figure 13 depicts details of FFM packaging design. A shell was constructed out of graphite fiber composite material with openings for the sun sensors, laser beacon, and IR photodetector. The IR detector was mounted on the analog board viewing outward along the FFM spin axis. Two sun sensors and the laser beacon viewed radially outward. A single sided digital board was mounted directly on top of the analog board separated by spacers. The digital board sat on a ledge within the graphite composite shell. It allowed passage of wires and coaxial cables through cuts on its edge. The magnetometer was placed in the middle of a methyl methacrylate impregnated lithographic material ("science cup") and was glued directly on the top of the digital board. Cavities inside the "science cup" mechanically supported the sun sensors and the laser beacon. Also additional cavities housed TCXO box and three shielded compartments of the RF transmitter. Seven (7) battery cells and four (4) wedges were tucked in between the "science cup" and the shell. Openings were allowed for the passage of all wires and coaxial cables. The final stages of the RF transmitter were placed near the top board of the magnetometer and under the antenna. The antenna was fastened to the "science cup" inserts from the top. A double sided copper tape wrapped along the edges of the antenna joined the antenna to the inner walls of the graphite composite shell. It shielded internal RF circuitry and cables from antenna radiation spill-over. The FFM flight units were vibrated to the flight acceptance levels at JPL prior to final delivery. The FFM units were dynamically spin balanced and mass imbalances were corrected by added weights.

### **Conclusion**

We have described the design, fabrication, and tests of all FFM subsystems in the context of the Enstrophy mission. Detailed information on the digital data subsystem design, FFM system design, the Enstrophy mission, and the associated scientific data reduction and their interpretations will be presented in the future.

Directions for future FFM system development will include fabrication of a monolithic magnetometer integrated with a low-magnetic-signature ASIC and an appropriate attitude determination subsystem.

### **Acknowledgement**

A portion of this work was performed by the Center for Space Microelectronics Technology and Solar System Exploration Program, Jet Propulsion Laboratory, California Institute of Technology, and was sponsored by the National Aeronautics and Space Administration. We also like to thank D. Hepner (USARL, Aberdeen Proving Ground); C. Cruzan, E. Cutting, S.

DiStefano, J. Drapou, C. Greenhall, T. McCann, J. Rademacher, D. Wallace (JPL); D. Rau, M. Widholm (University of New Hampshire); T. Stirling, C. Lankford (NASA Wallops); and the Enstrophy integration team at Poker Flat, Alaska for their support.

## References

1. R. Goldstein, M. Boehm, K.A. Lynch, H. Javadi, R.A. Wallace, "Autonomous, free-flying nano-spacecraft fleets for space physics measurements", *To be presented in the American Geophysical Union 1999 Spring Meeting, Special Session on New Missions.*
2. K.A. Lynch, Y. Zheng, R. Arnoldy, M. Boehm, R. Goldstein, H. Javadi, P. Kintner, P. Schuck, E. Klatt, H. Stenbaek-Nielsen, T. Hallinan, L. Peticolas, "Multiple Free-Flyer Magnetometer Measurements of Auroral Electric Currents: Results from the Enstrophy Sounding Rocket Mission", *To be presented in the American Geophysical Union 1999 Spring Meeting.*
3. M. Boehm, Y. Zheng, K.A. Lynch, R. Goldstein, H. Javadi, "Analysis of Enstrophy Sounding Rocket Free-Flyer Magnetometer Data: Techniques, Accuracy, and Results", *To be presented in the American Geophysical Union 1999 Spring Meeting.*
4. B. Blaes, H. Javadi, H. Spencer, "Free Flying Magnetometer Data Subsystem", *To be presented in the 13th Annual AIAA / Utah State University Conference on Small Satellites, Aug. 1999.*
5. Cardinal Components, Inc., 155 Route 46 West, Wayne, New Jersey 07470.
6. MicroPulse, Inc., 409 Calle San Pablo, Camarillo, CA 93012.
7. Eagle Picher Industries, Inc., C&Porter Streets, Joplin, MO 64804.
8. US Army Research Laboratory, Aberdeen Proving Ground, MD 21005



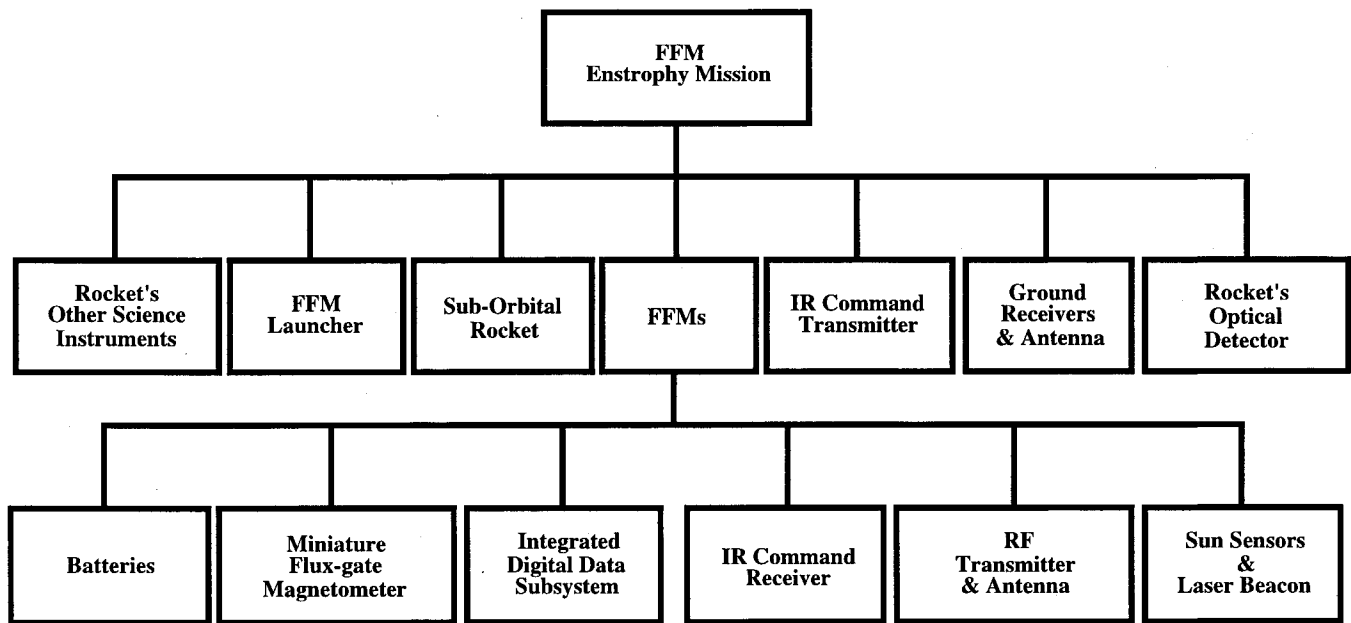


Figure 1- Enstrophy mission subsystem-level block diagram

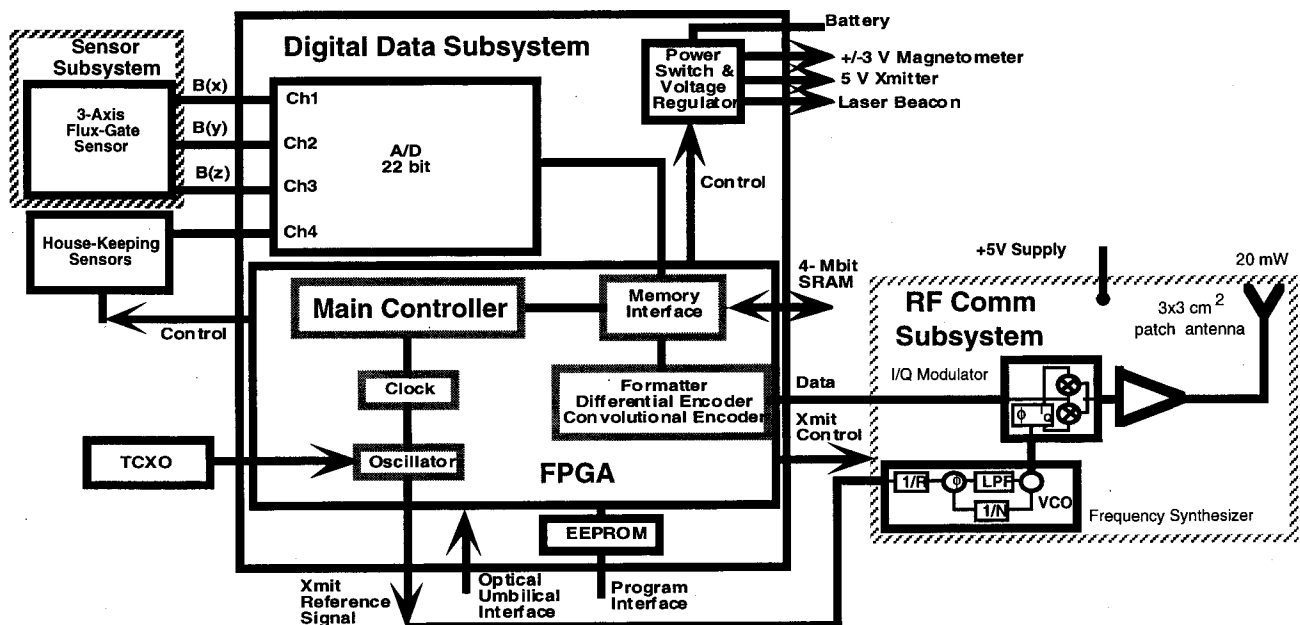
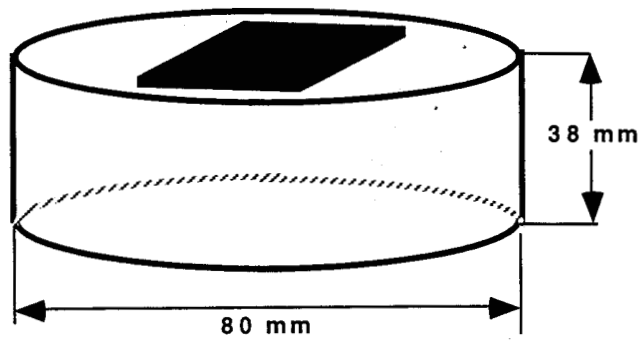
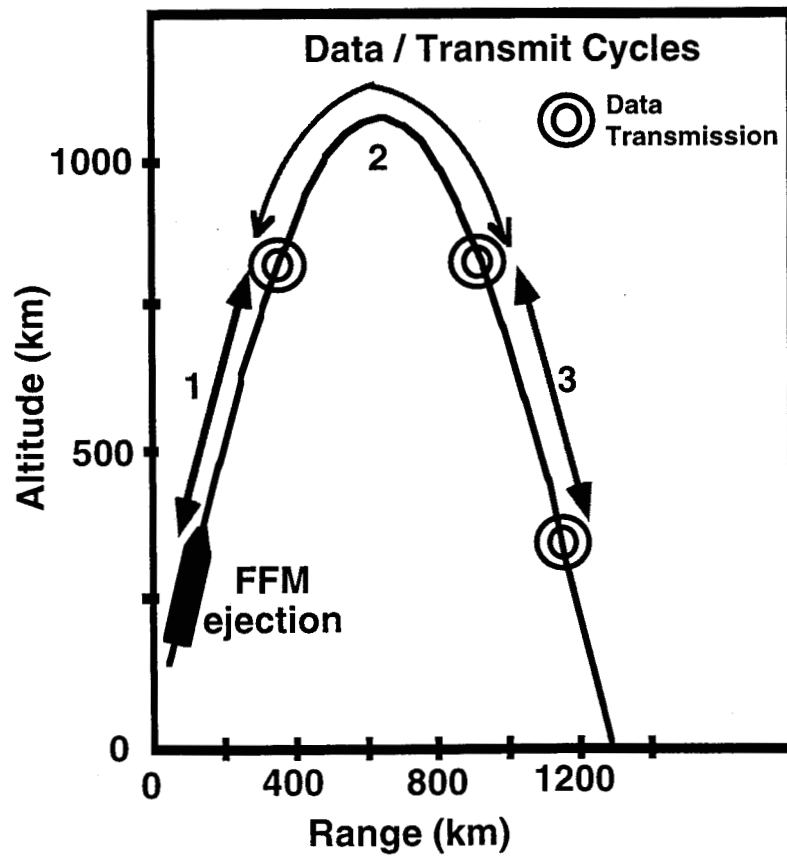


Figure 2- The block diagram of the FFM unit.





**Figure 3-** The mechanical structure envelope of the FFM unit.



**Figure 4-** Black Brant - 10 trajectory and Enstrophy Mission scenario.

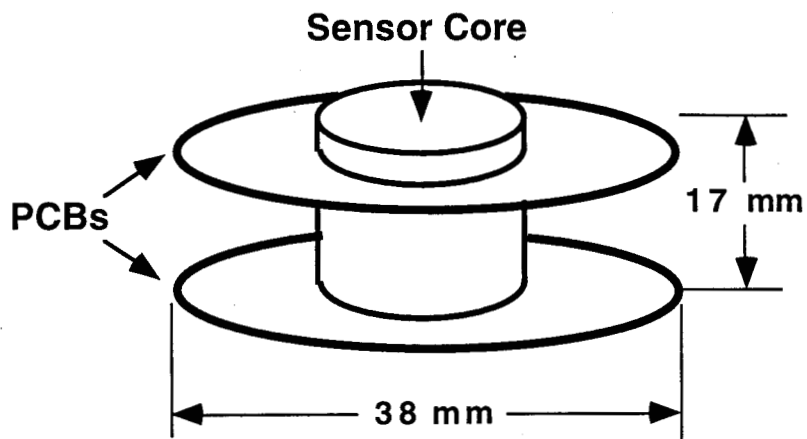


**Figure 5-** Sketch of the FFM miniature fluxgate magnetometer (Applied Physics System).

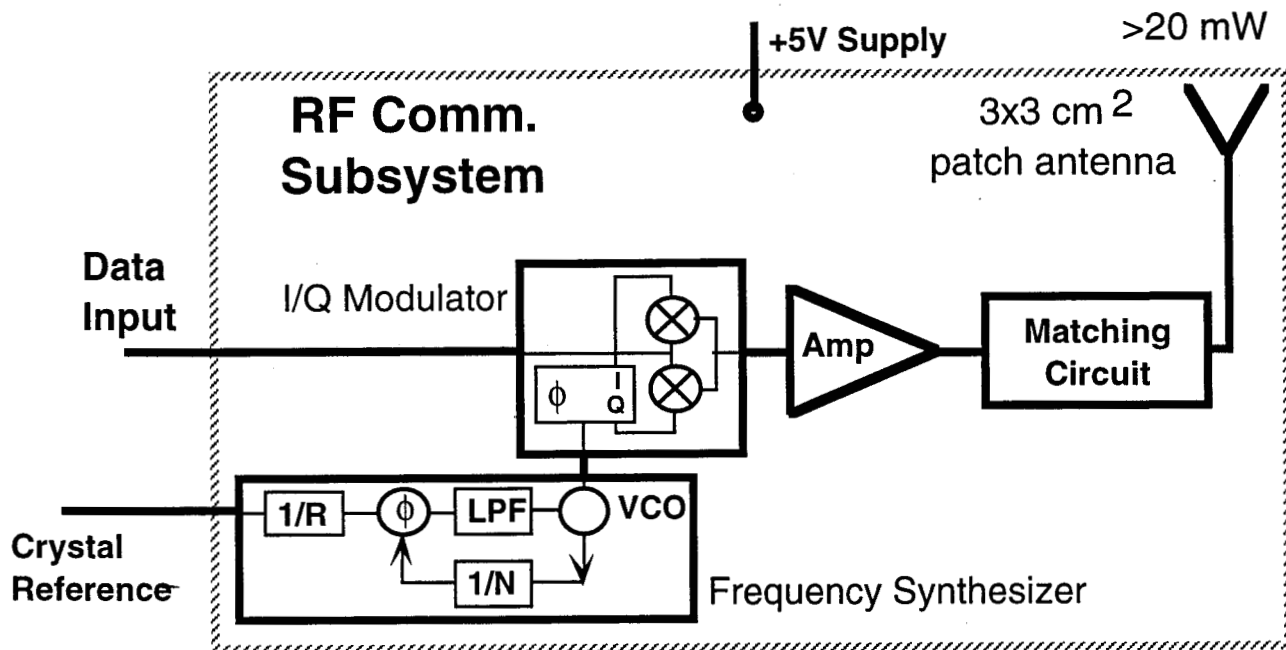


**Figure 6-** Block diagram of the FFM S-band transmitter with the connected antenna.

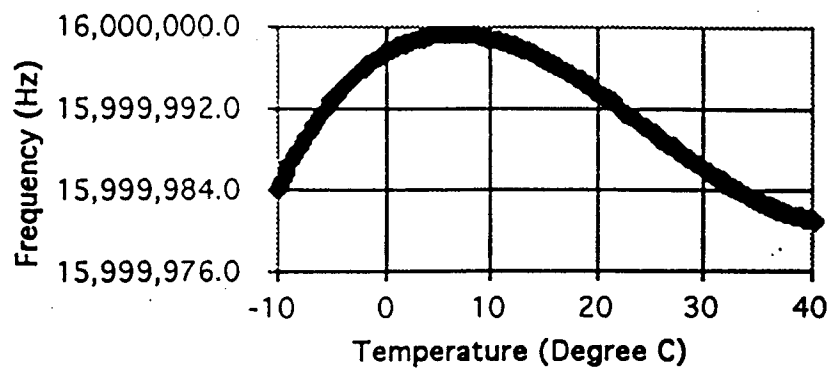


Figure 7- Temperature dependence of the FFM 16 MHz TCXO

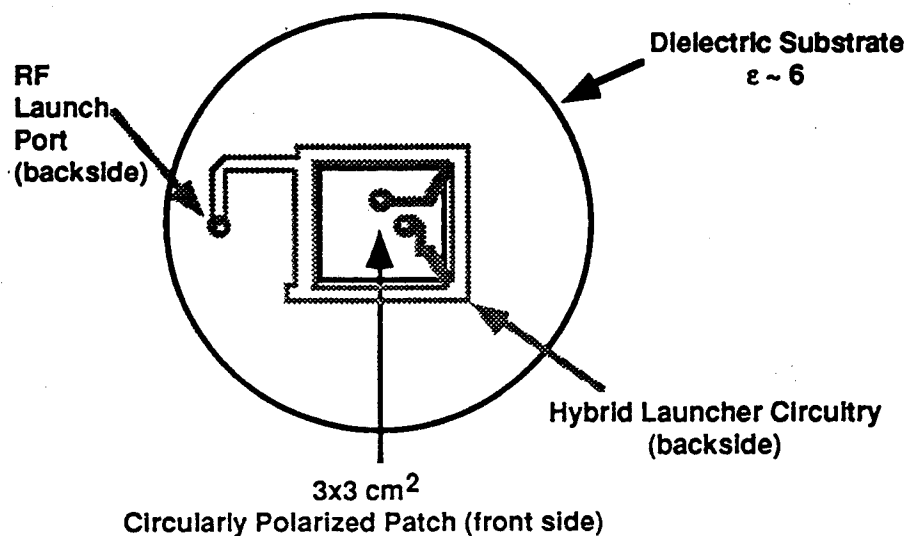


Figure 8- Schematic of the FFM single patch antenna, its hybrid launcher, and feed points

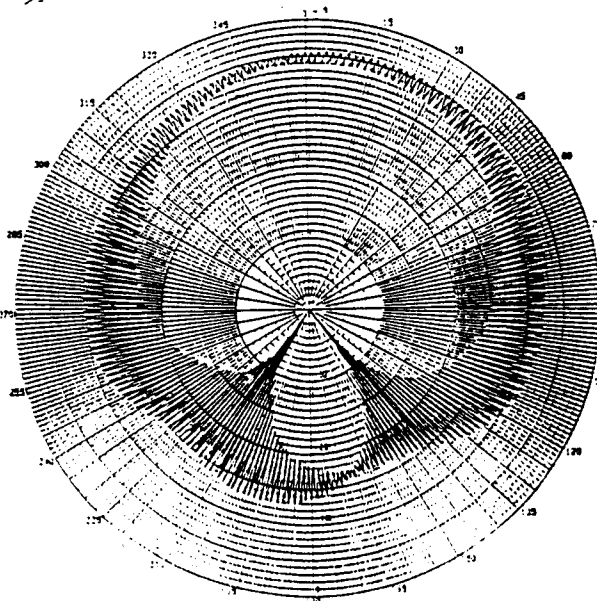
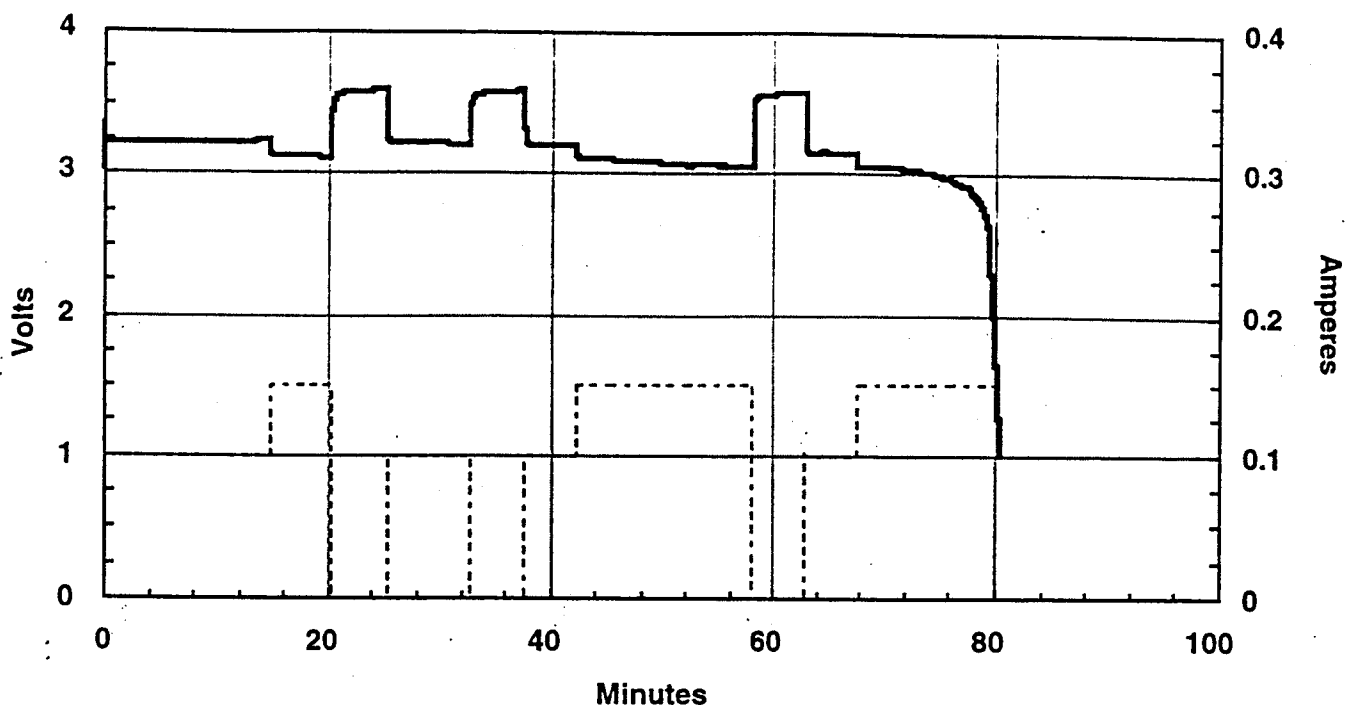
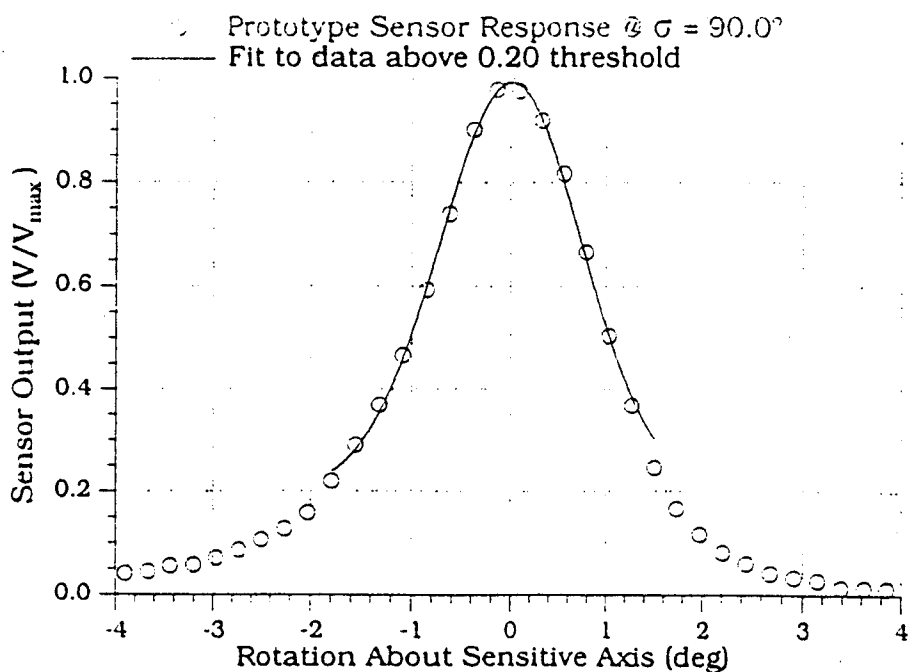


Figure 9- A typical FFM unit antenna radiation pattern.



**Figure 10-** Capacity measurement of a single LTC-312 battery vs time at 25° C. The wide solid line is the battery voltage and the dashed line is the load current. The load represents worst-case power consumption for any of the 7 flight batteries inside a FFM. The current load includes all pre-flight tests, nightly tests at Poker Flat, and one full mission (preceded with ~ 5 minutes delay between when the FFM power is turned on till the magnetometer is powered). The graph shows that the FFM battery can support almost one additional full mission at 25° C. The current levels have more than 50% margin.



**Figure 11-** A typical amplitude variation of a FFM sun sensor for rotation about the axis normal to the slit opening in the plane perpendicular to the slit.

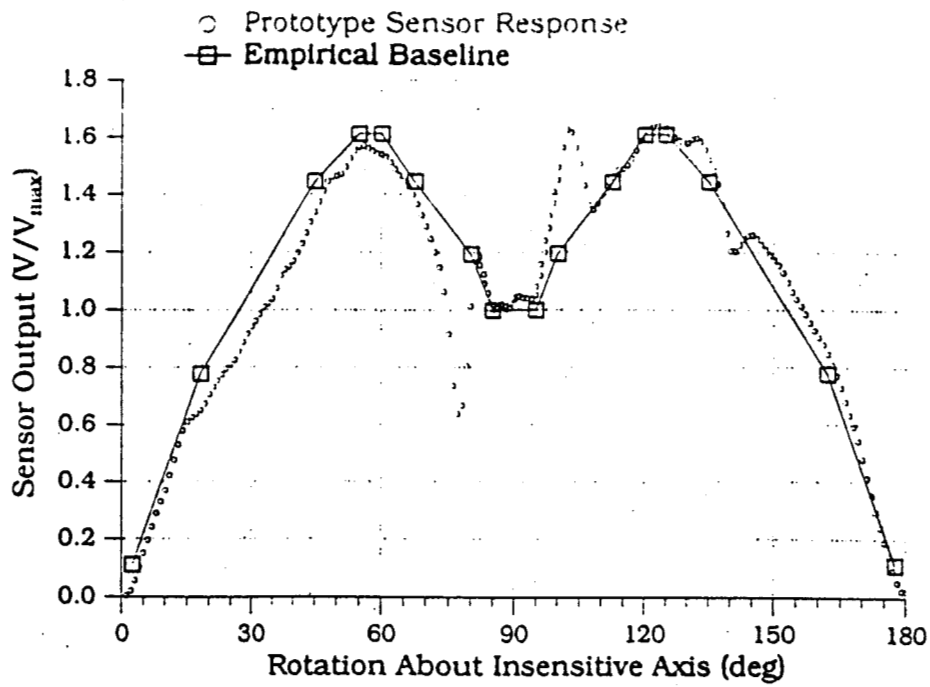


**Figure 12-** A typical amplitude variation of a FFM sun sensor for rotation about the axis normal to the slit opening in the plane parallel to the slit.

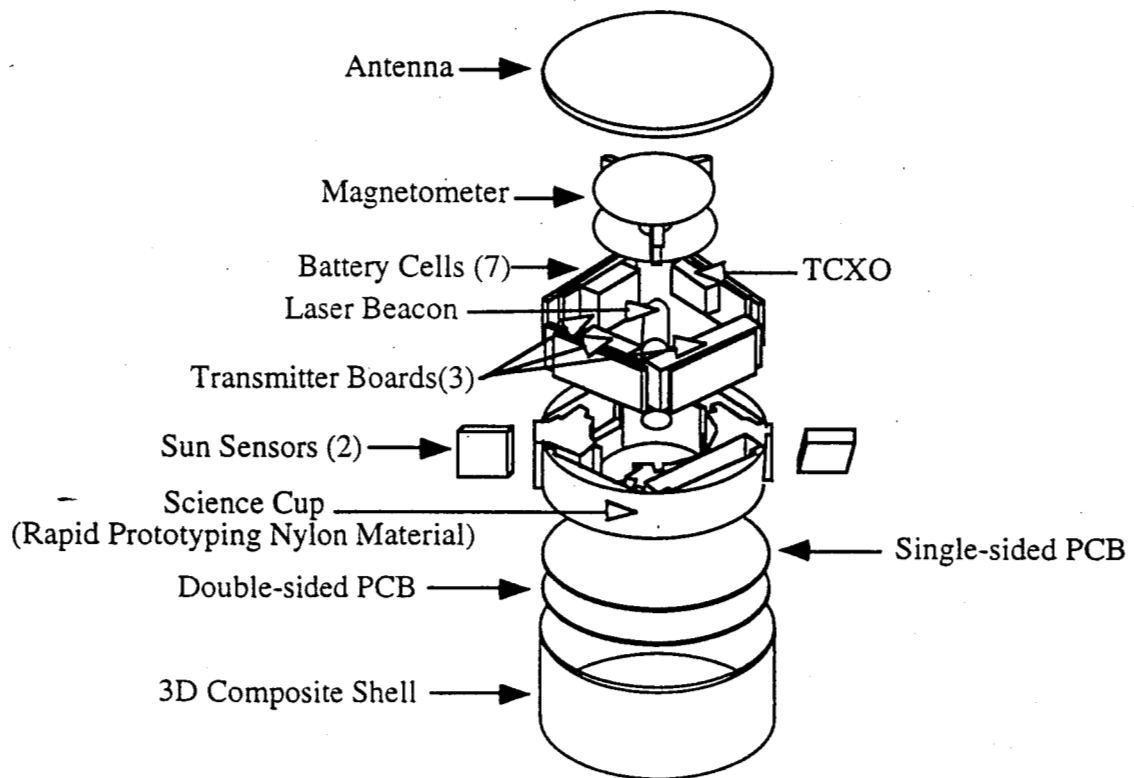


**Figure 13-** Exploded view of the FFM flight unit.